Analyst

The selective electrochemical detection of homocysteine in the presence of glutathione, cysteine, and ascorbic acid using carbon electrodes

Journal:	*Analyst*
Manuscript ID:	AN-ART-02-2014-000372.R1
Article Type:	Paper
Date Submitted by the Author:	09-Apr-2014
Complete List of Authors:	Lee, Patricia; Oxford University, Department of Chemistry Lowinsohn, Denise; Instituto de Ciências Exatas, Chemistry Compton, Richard; Oxford University, Department of Chemistry

The selective electrochemical detection of homocysteine in the presence of glutathione, cysteine, and ascorbic acid using carbon electrodes

P. T. Lee[1], D. Lowinsohn[1, 2], R. G. Compton[1]*

[1]Department of Chemistry, Physical and Theoretical Chemistry Laboratory, Oxford University, South Parks Road, Oxford, OX1 3QZ, United Kingdom

[2]Department of Chemistry, Instituto de Ciências Exatas, Universidade Federal de Juiz de Fora, 36036-330, Juiz de Fora, MG, Brazil.

*Corresponding author: richard.compton@chem.ox.ac.uk.

Article submission to 'Analyst'.

Abstract

The detection of homocysteine, HCys, was achieved with the use of catechol via 1,4-Michael addition reaction at carbon electrodes: glassy carbon electrode and carbon nanotube modified glassy carbon electrode. The selective detection of homocysteine was investigated and achieved in the absence and presence of glutathione, cysteine and ascorbic acid using cyclic voltammetry and square wave voltammetry. A calibration curve of homocysteine detection was determined and the sensitivity is (0.20 ± 0.02) μA μM^{-1} and limit of detection is 660 nM within the linear range. Lastly, the use of commercially available multi walled carbon nanotube screen printed electrodes was applied to the system for selective homocysteine detection. This work presents a potential practical application

towards medical applications as it can be highly beneficial towards quality healthcare management.

Keywords: catechol, thiols, *ortho*-quinone, homocysteine, carbon nanotube, glassy carbon electrode, carbon electrodes, 1,4-Michael addition reaction, screen printed electrodes

1. Introduction

Homocysteine, HCys (figure 1a), an antioxidant, is a thiol containing non-protein amino acid that partakes in biological functions that maintains metabolism [1]. It was first hypothesized in the 1960's that increased levels of homocysteine may lead to implications to leukemia[2, 3], Alzheimer's disease[4, 5], cancer[2] and cardiovascular diseases[1, 4, 6] such as atherosclerosis[1, 6], arterial disease[1, 7], and atherothrombotic vascular disease[6, 7]. Though a typical range of homocysteine in healthy blood plasma is 5 – 15 µM [1, 8, 9]; studies have shown that elevated levels of homocysteine, ≥ 15 µM, can lead to any of the three classification of hyperhomocystienemia which is a high risk factor for the diseases mentioned above. The three classifications of hyperhomocyteinemia are mild (15 – 30 µM), intermediate (30 - 100 µM), and severe (≥ 100µM)[1, 9-14].

Some methods of homocysteine detection include chromatography coupled with spectroscopy[4, 5, 9, 15, 16], fluorescence[4, 9], immunoassay [4, 5, 7, 9], and electrochemistry [9, 16, 17]. However, the use of analytical instrumentations has its drawbacks with it being expensive, time consuming, and requiring technical training and handling. The use of electroanalytical methods in the form of dedicated sensors have major advantages over the detection methodologies mentioned above since measurements can be fast, easy and performed without any separation or purification of the sample[9, 16, 17]. Though, the problem with the

direct electrochemical detection is the poor voltammetric responses on conventional bare electrode surface due to the large oxidation over potential of homocysteine[9, 17] (*ca*. + 0.40 V vs. SCE). By developing a quick and easy monitoring system of homocysteine levels in biological samples, it would be advantageous for early disease detection or research-based instrumentation.

Salehzadeh et al. [16] were the first to report the selective detection of homocysteine in the presence of cysteine and glutathione in a partly *non-aqueous* system only using 3,5-di-tert-butylcatechol at glassy carbon and carbon nanotube modified carbon electrodes. They observed that cysteine did not interfere but used 3,5-di-tert-butylcyclohexa-3,5-diene-1,2-dione to react with glutathione to eliminate it as an interference. The purpose of our paper is to present a simple electrochemical method to selectively detect homocysteine also in the presence of cysteine and glutathione. In contrast to Salehzadeh et al., the detection was achieved solely in the presence of catechol, which is readily soluble in 100% aqueous systems, again using glassy carbon and carbon nanotube modified carbon electrodes. Cyclic voltammetry and square wave voltammetry were thus used without the need for extensive pre-treatment to the sample. Further, we extend the method to embrace screen printed electrodes. To the best of our knowledge, no other modified electrodes for the selective detection of homocysteine have been reported.

Carbon electrodes are widely used in electroanalysis as they have a relatively low cost compared to the precious metal electrode, chemical inertness, and provide a wide potential range in aqueous solutions[18, 19]. Catechol (figure 1b) was chosen to react with the thiol containing molecule to facilitate the detection of homocysteine. The reaction between o-quinone and thiols has been reported in literature[16, 20-25] where there are two possible

reaction pathways that can occur[21, 22]: one being an electrocatalytic reaction and the second, 1,4-Michael addition reaction. An electrocatalytic reaction involves the electrochemically oxidized *ortho*-quinone undergoing a two electron, two proton process to reduce the thiol-containing species, RSH, into a disulfide, RSSR[20].

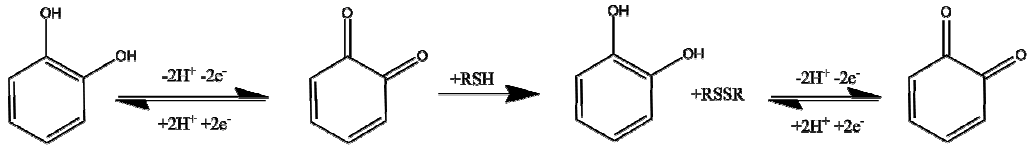

(1)

The reaction regenerates the starting catechol so will continue catalytically until two electrons per RSSR formed due to the *ortho*-quinone being able to electrochemically re-oxdize itself from the electrons provided by the electrode. The cyclic voltammogram will show in an increase in the forward peak and a decrease in the back peak as the concentration of the thiol species increases. For the second type of reaction, the *ortho*-quinone may undergo a 1,4-Michael addition reaction as the thiol performs a nucleophillic attack on the oxidized *ortho*-quinone species resulting in a new electrochemical species[20, 21]. This type of reaction will initially involve a two electron, two proton process to oxidize the catechol then an additional two electrons will be required for the nucleophillic attack to take place thus involving a net total of four electron process.

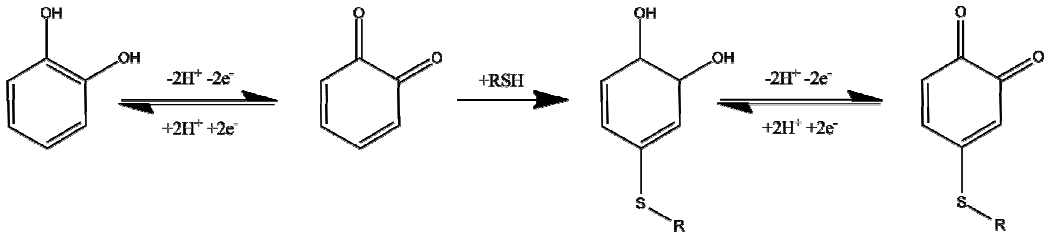

(2)

The voltammogram can show a forward peak increasing as the back peak decreasing with increasing concentration of thiol species; in addition, the attack on the *o*-quinone species by

a thiol can result in an introduction of a new peak away from its parent peak potential. This paper will present a method towards homocysteine detection using a catechol via 1,4-Michael addition reaction at the carbon nanotube modified glassy carbon electrode.

2. Experimental Procedure

2.1. Reagents

All reagents were purchased through Sigma-Aldrich and Lancaster Synthesis at their highest available purity and were used as received without any further purification steps; catechol (99%, Aldrich), glutathione (98%, Sigma-Aldrich), D,L-cysteine (97%, Lancaster Synthesis), D,L-homocysteine (≥95%, Sigma), and ascorbic acid (99%, Aldrich). The bamboo-like multi-walled carbon nanotubes, MWCNT (30 ± 10 nm diameter, 5 - 20 μM length, > 95% purity) were purchased from Nanolab, Waltham, MA, USA. The bamboo-like carbon nanotubes were characterized by the manufacturer using transmission electron microscopy (TEM). All solutions were prepared with deionized water at a resistivity of no less than 18.2 MΩ cm^{-1} at 25˚C (Millipore, UK). The buffer solutions, 0.15 M, were prepared using potassium monohydrogen phosphate (K_2HPO_4) (≥98%, Sigma-Aldrich), potassium dihydrogen phosphate (KH_2PO_4) (≥99%, Sigma-Aldrich), and potassium hydroxide (KOH) (≥85%, Sigma-Aldrich) accordingly to the required pH range. All buffer solutions were freshly made prior to experiments with supporting electrolyte of 0.10 M potassium chloride (KCl) (99%, Sigma-Aldrich) added to each solution.

2.2. Apparatus

The electrochemical experiments were carried out in a three electrode system using a saturated calomel electrode, SCE, reference electrode (Hach Lange, UK), a platinum mesh

99.99% (Goodfellow, UK) counter electrode, and a glassy carbon electrode, GCE, (CH Instruments, USA) working electrode is used as the basis of the modified electrode which will be discussed in a later section. The surface area of the bare glassy carbon electrode is 0.071 cm^2. All experiments were conducted using a computer controlled potentiostat, PGSTAT 101 (ECO-chemie, NL). A temperature controlled bath was also used to ensure that all electrochemical experiments were carried out at (20 ± 2) ˚C in a Faraday cage. All pH measurements were conducted using a pH213 Microprocessor pH meter (Hanna instruments, UK). The pH meter was calibrated using Duracal buffers of pH 4.01 ± 0.01, pH 7.00 ± .001, and pH 10.01 ± 0.01 (Hamiliton, CH).

2.3. Preparation of modified carbon nanotube glassy carbon electrode (CNT-GCE)

The modification of the electrode is the following, as it was freshly prepared at the start of each experiment. The GCE was first polished with sequentially 3.0, 1.0, and 0.1 µm diamond spray (Kemet, UK) then rinsed with ethanol and de-ionized water. Afterwards, the carbon nanotubes were immobilized onto the surface of the glassy carbon electrode through drop casting method. The drop casting method is essentially dropping an aliquot of a CNT-ethanol suspension (0.1 mg / mL) over the surface of the GCE. This allows the ethanol to evaporate at room temperature thus leaving a layer of CNT at the electrode surface. To ensure a full suspension of the CNT-ethanol, the solution was briefly sonicated using a sonication bath prior to drop casting. A total of 6.0 µg of CNT was drop casted onto the GCE during the modification of the electrode. The surface area of the modified CNT-GCE was obtained by cyclic voltammetry at different scan rates, ranging from 25 mVs^{-1} to 400 mVs^{-1}, in 1.0 mM hexaammineruthenium(III) chloride and 0.1 M potassium chloride solution. The calculated average surface area for the CNT-GCE is (0.23 ± 0.02) cm^2.

2.4. *Screen printed electrodes*

The use of multi-walled carbon nanotube screen printed electrodes, CNT-SPE, and graphite screen printed electrodes, G-SPE, were applied. The disposable screen printed electrodes were acquired from DropSens (Spain) which has a ceramic substrate consisting of a multi-walled carbon nanotube or graphite working electrode, a carbon counter electrode and a silver reference electrode. The characterization using scanning electron microscopy (SEM) of these screen printed electrodes can be found on their website[26].

3. **Results and Discussion**

3.1. *Electrochemical characterization of catechol*

Cyclic voltammograms of the system were taken at different scan rates ranging from 25 mVs^{-1} to 400 mVs^{-1} in PBS, pH7.0 at 20°C (figure 2) to initially characterize the electrochemical behaviour of 0.1 mM catechol using at both CNTs-GCE and GCE. The figure shows the redox process of catechol at $E_{1/2}$ = + 0.15 V (vs. SCE). This is attributed to the two electron, two proton oxidation of the catechol to the corresponding *ortho*-quinone species[21, 22, 27, 28]:

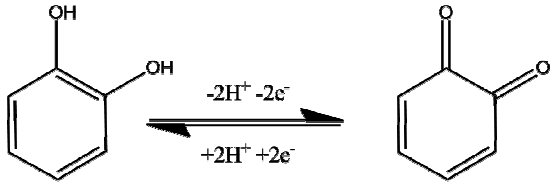

(3)

The inset in figure 2 shows that there is a linear correlation when the peak current, i_p, is plotted with the square root of scan rate, $v^{1/2}$, suggesting a diffusional process of catechol at either electrode. The diffusion coefficient was estimated using the Randle-Ševčik

equation, as being (7.0 ± 1.0) x 10^{-6} cm^2s^{-1} for the CNTs-GCE and 7.5 x 10^{-6} cm^2s^{-1} for GCE, this is reasonably consistent with the literature value[28, 29], 7.7 x 10^{-6} cm^2s^{-1}.

3.2. Catechol electrochemical characterization in the presence of homocysteine

Cyclic voltammetry (50 mVs^{-1}) was used to observe the electrochemical response of 0.1 mM catechol (pH 7.0, PBS) in a presence of HCys. Figure 3 shows the comparison of the voltammetric response of the catechol in the absence (dotted line) and presence (solid line) of 0.1 mM HCys at the CNTs-GCE (i) and GCE (ii). In the presence, the voltammogram shows the forward peak increases as the back peak decreases and a new product peak emerges at *ca.* - 0.20 V (vs. SCE). This peak is due to the reduction of substituted catechol molecule[20], as described above in equation 2.

3.3. Electrochemical detection of homocysteine

To observe the electrochemical behaviour of catechol with different concentrations of homocysteine, cyclic voltammetry (scan rate of 50 mVs^{-1}) was carried out with a solution containing 0.1 mM catechol at varying homocysteine concentrations ranging from 0 – 0.1 mM. Figure 4 shows that as the concentration of homocysteine increases, the forward and new product peak, *ca.* - 0.20 V (vs. SCE), increases as the back peak decreases. When the peak current of the new product peak is plotted with concentration of homocysteine (figure 4 inset), the linear trend increases up to 60 µM and then decreases at 0.1 mM homocysteine. This suggests that there is a maximum concentration of homocysteine that will be able to react with the concentration of catechol available in solution. However, the systematically increasing trend shows the possibility of homocysteine detection.

To increase the sensitivity of HCys detection in the presence of 0.1 mM catechol (PBS, pH 7.0), square wave voltammetry was utilized. The parameters were optimized for CNT-GCE and GCE at frequency 50 Hz, step potential 4.0 mV, and amplitude 50 mV. Figure 5 shows the square wave voltammograms of the catechol response to different concentrations of homocysteine at the CNT-GCE as we observe similar response at GCE. The results obtained with square wave voltammetry are consistent with the results obtained with cyclic voltammetry for both electrodes; where the catechol peak (*ca.* +0.14 V vs. SCE) decreases and the new product peak at *ca.* -0.20 V (vs. SCE) emerges and grows with increasing homocysteine concentration. There is a linear relationship when the peak current of the product, *ca.* -0.20 V (vs. SCE), is plotted with concentration of homocysteine. For CNT-GCE, the linear relationship is I(μA) = 0.2[HCys](μM) with concentrations up to 80 µM (figure 5 inset) and the limit of detection (LOD) was determined to be 120 nM. For GCE, the linear relationship is I(μA) = 0.2[HCys](μM) at homocysteine concentration up to 40 µM and a determined LOD of 90 nM.

3.4. Interference studies

Towards the use of homocysteine detection in authentic biological samples and media, the selectivity of the system was next investigated at each electrode. First, an individual assay with 0.1 mM catechol (PBS, pH 7.0) was done with the separate additions of 0.1 mM of each antioxidant: glutathione (GSH), cysteine (Cys), and ascorbic acid (AA) at each CNT-GCE and GCE. These antioxidants were chosen because they are commonly found in biological samples at high concentrations (table 1) [14, 22, 30-41] and have a high propensity to interact with *ortho*-quinones[21, 23, 32, 42, 43]. In addition, 0.1 mM of each analyte was use to

present the worst-case scenario of possibly having abnormally high concentrations present in biological samples[14, 22, 30-41].

3.4.1. Interference study at the glassy carbon electrode

Cyclic voltammograms (50 mVs^{-1}) were taken of 0.1 mM catechol (PBS, pH 7.0) solutions containing 0.1 mM of each GSH, Cys, and AA. Figure 6 shows a cyclic voltammogram comparison in the absence (curve a) and presence (curve b) of these antioxidants: GSH (i), Cys (ii) and AA (iii) reacting with catechol. For GSH and Cys, the voltammograms show the forward peak increases and back peak decreases but only in the case with GSH, a new peak emerges at *ca.* - 0.20 V (*vs.* SCE) due to the catechol-thiol interaction favouring the 1,4-Michael addition reaction. In the case with the catechol interaction with Cys at the GCE, the favouring reaction seems to be electrocatalytic at the GCE. With AA, the voltammogram shows that the forward peak increases slightly and new peak emerges ca. 0 V (vs. SCE) indicating that it is the oxidation of pure ascorbic acid at the GCE. Upon examining all the voltammograms, there can be difficulties measuring HCys when in the presence of GSH at GCE because the peak potentials of their adduct with oxidized quinones are close to each other.

3.4.2. Interference study at the carbon nanotube modified carbon electrode

Figure 6 shows the electrochemical response at each electrode of 0.1 mM catechol (dotted line) in a presence of 0.1 mM of each antioxidants (solid lines): GSH (i), Cys (ii), and AA (iii) at the CNT-GCE. Voltammograms show an increase in forward peak with a decrease in the back peak for catechol reacting with GSH (i) and Cys (ii), with an introduction of a new product peak at *ca.* - 0.200 V, and +0.300 V respectively. This introduction of a new product

peak indicates a 1,4-Michael addition reaction is favoured and occurs with the thiols at the CNT-GCE. While there was no new product peak for the presence of ascorbic acid, the voltammogram show a slight increase in the forward peak which is similarly seen with GCE. By examining the peak potentials of the new product peak, the presence of glutathione can be a possible interference towards the detection of homocysteine as the product peak potentials are close to each other. For the case with cysteine, the product peak emerges at a different peak potential further away from the reaction with homocysteine and glutathione. It is suspected that the catechol reaction with each different thiol reacts to form a new electrochemical species different from each other thus having different peak potentials.

3.4.3. Homocysteine selectivity

At this point, it would be difficult to quantify homocysteine in the presence of glutathione with the square wave voltammetry parameters presented above (section 3.3) at either electrodes. Figure 7 shows the behaviour of catechol in the presence of homocysteine (curve a), glutathione (curve b), and both (curve c) at 50 mVs^{-1}, similar behaviour is also seen at GCE. Notice that in the presence of both HCys and GSH (figure 7c); the new product peaks for both analytes are close which makes it difficult to determine changes in peak current between the two analytes, if it should occur. As an attempt to optimize the single homocysteine signal, one proposed method can be to take advantage of the different molecular size and reaction rates of either analytes with catechol. The aim would be to apply a higher scan rate to outrun the glutathione-catechol reaction but still be able to allow the homocysteine-catechol interaction to take place.

Figure 8 shows cyclic voltammetry at an optimum scan rate at 1.5 Vs^{-1} for GCE (i) and 500 mVs^{-1} for CNTs-GCE (ii) was found and applied to a catechol solution with the presence of glutathione (curve a) and homocysteine (curve b) (PBS, pH 7.0) separately to see the possibility of homocysteine selectivity. There is no significant signal for the product peak of the glutathione-catechol reaction (curve a) while for the homocysteine-catechol reaction (curve b), the product peak (*ca*. - 0.20 V vs. SCE) emerges for both systems. This indicates that it is possible to detect homocysteine in the presence of glutathione at the higher scan rate. As mentioned before, AA and Cys were not interferences to the homocysteine product signal and now, it can be possible to have homocysteine detection in the presence of AA, Cys and GSH using cyclic voltammetry.

Square wave voltammetry (optimized for CNT-GCE at frequency 50 Hz, amplitude 50 mV, and step potential 10 mV and GCE at frequency 50 Hz, amplitude 75 mV, and step potential 30 mV) was applied to a solution containing various HCys concentrations, 0 – 0.1 mM, in a presence 0.1 mM of each catechol, GSH, Cys, and AA. Figure 9 shows the square wave voltammograms of different homocysteine concentration in the presence of cysteine, glutathione and ascorbic acid at the CNT-GCE. The inset to figure 9 shows the homocysteine-catechol product current peak increases with homocysteine concentration at both electrodes. Homocysteine selectivity was not achieved at GCE under the optimized square wave voltammetry parameters presented because the result shows a signal in the absence of homocysteine due to catechol-glutathione product. While the selectivity of homocysteine was successfully achieved at CNT-GCE as no signal appeared in the absence of homocysteine when the other antioxidants are present. The differences in selectivity can be rationalized by the diffusion changes at the electrode surfaces, bare glassy carbon electrode versus

porous layer of carbon nanotube modified electrode[44, 45]. The porous layer is likely to promote the glutathione and quinone reaction. Under linear diffusion semi-infinite diffusion conditions the reaction is too slow to be usefully observed whereas the 'thin layer' like environment in the porous layer slows the transport and hence help aide the reaction. Therefore, the CNT-GCE is the best electrode at this time to obtain selective homocysteine detection in the presence of glutathione, cysteine and ascorbic acid.

Sensitivity of homocysteine at CNT-GCE was obtained in the presence of these analytes, at the range 0 – 10 μM, is (0.20 ± 0.02) μA μM^{-1} and the limit of detection is determined to be 660 nM. It is suspected that the narrow working range is due to the antioxidants present; including homocysteine, undergo a competition reaction with the available catechol in solution. In spite of the antioxidant present undergoing a reaction we can still observe no change in peak current up to 10 μM homocysteine in the presence of 0.1 mM analytes. However, there is a possibility that the dynamic range might be extended if those concentrations were lower.

3.5. Homocysteine detection using carbon nanotube screen-printed electrodes (CNT-SPE)

The use of readily available commercial carbon nanotube screen-printed electrodes, CNT-SPE, was applied to this system. CNT-SPE was tested in a solution containing 0.1 mM of catechol and all of the other analytes mentioned above while varying the concentration of homocysteine (pH 7.0, PBS) at 20˚C. To ensure the same potential and conditions used previously, SCE was used as the reference electrode in the testing for comparison to the CNT-GCE. Figure 10 shows a calibration curve of the tested CNT-SPE plotted in comparison with the other calibration curves of homocysteine concentration up to 10 μM. The figure

shows the linear range, 0 – 10 μM, with using CNT-SPE is similar to CNT-GCE in the presence of the other analytes. The sensitivity for HCys at CNT-SPE is (0.20 ± 0.02) μA μM^{-1} which is the same in the absence and presence of the analytes at CNT-GCE. Graphite screen-printed electrode was also applied to the same system. However, a signal appeared in the absence of homocysteine due to catechol-glutathione product showing that homocysteine selectivity is not possible under these conditions. To conclude, the commercially available carbon nanotube screen printed electrodes was shown to be applicable towards homocysteine detection.

4. **Conclusion**

The use of an electrochemically generated *ortho*-quinone facilitates the reaction of the thiol containing compound, homocysteine, on carbon electrodes. We have demonstrated that the detection of pure homocysteine is able to takes place using two different carbon electrodes, bare glassy carbon electrode and carbon nanotube modified carbon electrode. In the presence of other antioxidants: glutathione, cysteine and ascorbic acid, homocysteine selectivity was not possible at GCE. The selective detection of homocysteine was achieved using a carbon nanotube modified electrode with a sensitivity of (0.20 ± 0.02) μA μM^{-1} and a limit of detection 660 nM at a linear range of 0 – 10 μM in the absence and presence of other antioxidants: glutathione, ascorbic acid, and cysteine. In addition, the use of commercially available carbon nanotube screen printed electrodes was applied and it was shown that it can be applicable towards facile, fast and disposable electrodes for homocysteine detection.

Acknowledgement:

D. Lowinsohn thanks CAPES (Process 10080-12-0) for a post-doctoral fellowship.

Figures

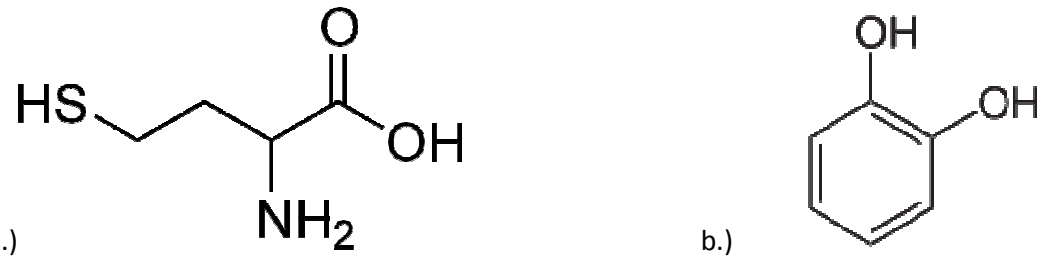

Figure 1. Chemical structure of a.) homocysteine b.) catechol.

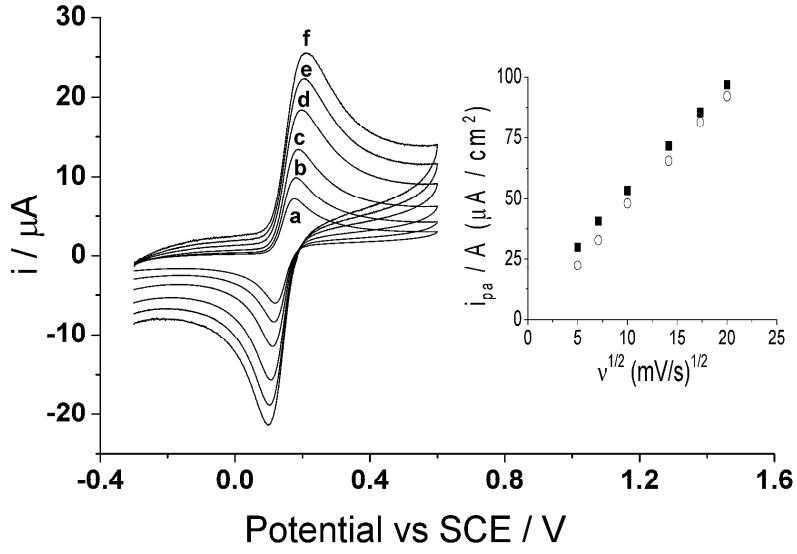

Figure 2. Cyclic voltammograms of CNT-GCE in 0.1 mM catechol (PBS, pH 7.0) at 20˚C **a.)** 25 mV s^{-1} **b.)** 50 mV s^{-1} **c.)** 100 mV s^{-1} **d.)** 200 mV s^{-1} **e.)** 300 mV s^{-1} **f.)** 400 mV s^{-1}. *Inset:* peak current, i_{pa}, vs. square root of scan rate, $v^{1/2}$. ■ CNT-GCE and **O** GCE.

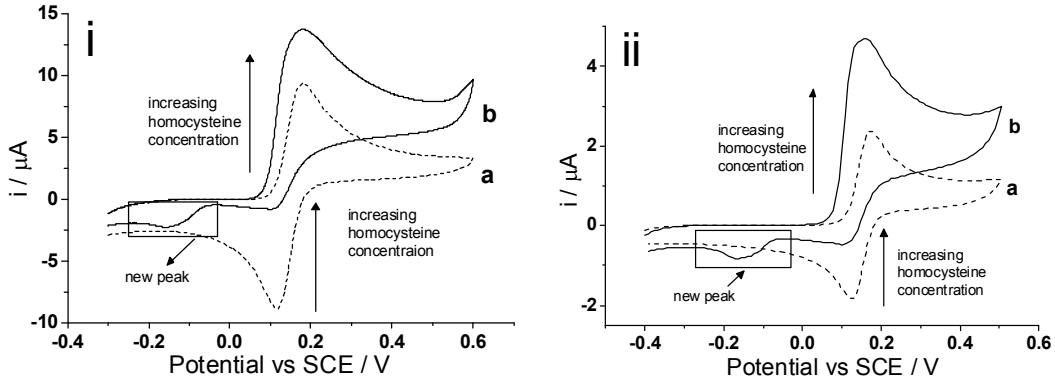

Figure 3. Cyclic voltammograms (50 mVs^{-1}, pH 7.0 phosphate buffer) illustrating the 0.1 mM catechol response in an absence (dotted) and presence of 0.1 mM homocysteine (solid) at the i.) CNT-GCE and ii.) GCE.

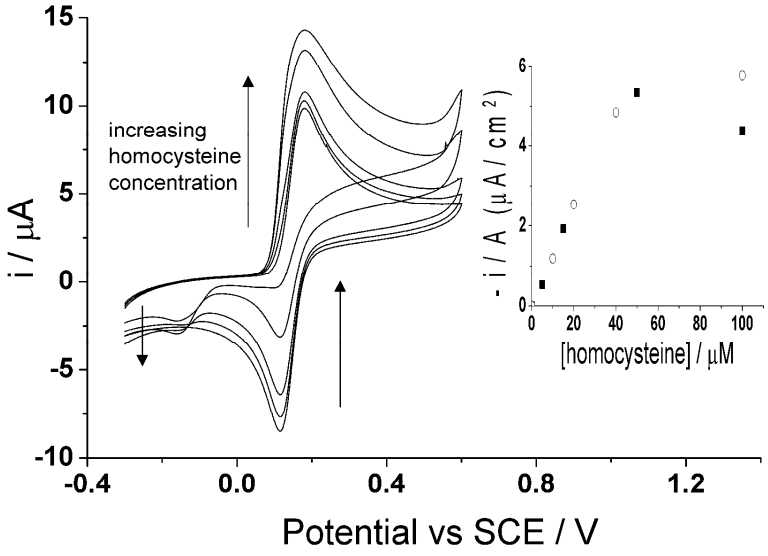

Figure 4. Cyclic voltammograms (50 mVs^{-1}, pH 7.0 phosphate buffer) illustrating the 0.1 mM catechol response to homocysteine concentrations ranging from 0 – 0.1 mM. *Inset:* peak current of the new peak plotted against the concentration of homocysteine. ■ CNT-GCE and O GCE.

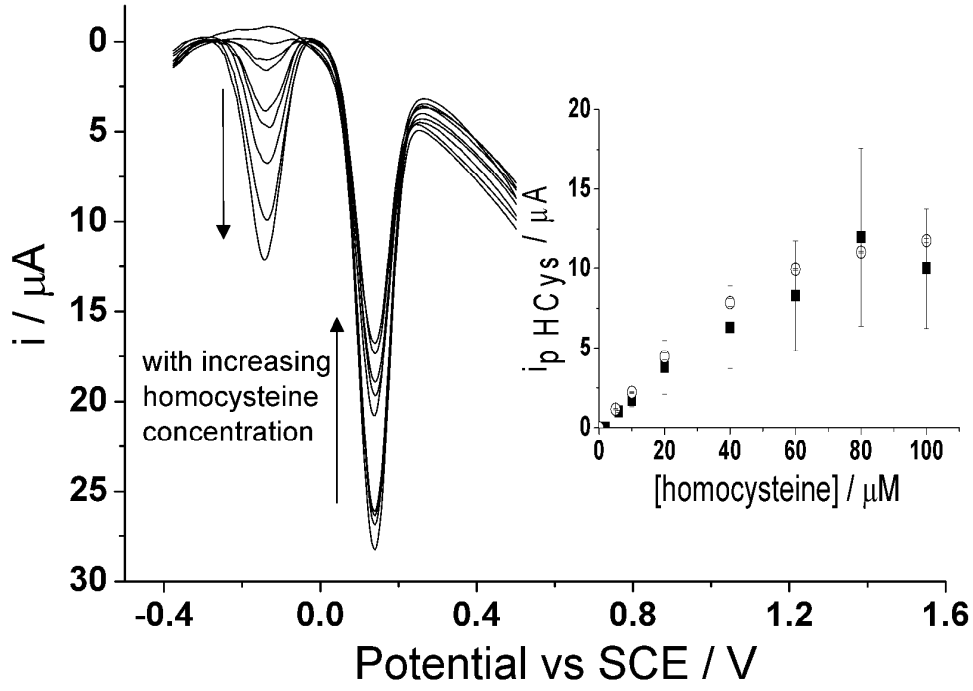

Figure 5. Square wave voltammetry response of 0.1 mM catechol at the CNT-GCE with varying concentration of homocysteine (PBS, pH 7.0) ranging from 0 – 0.1 mM. *Inset:* Peak current at *ca.* – 0.20 V (vs. SCE) plotted against concentration of homocysteine. ■ CNT-GCE and **O** GCE.

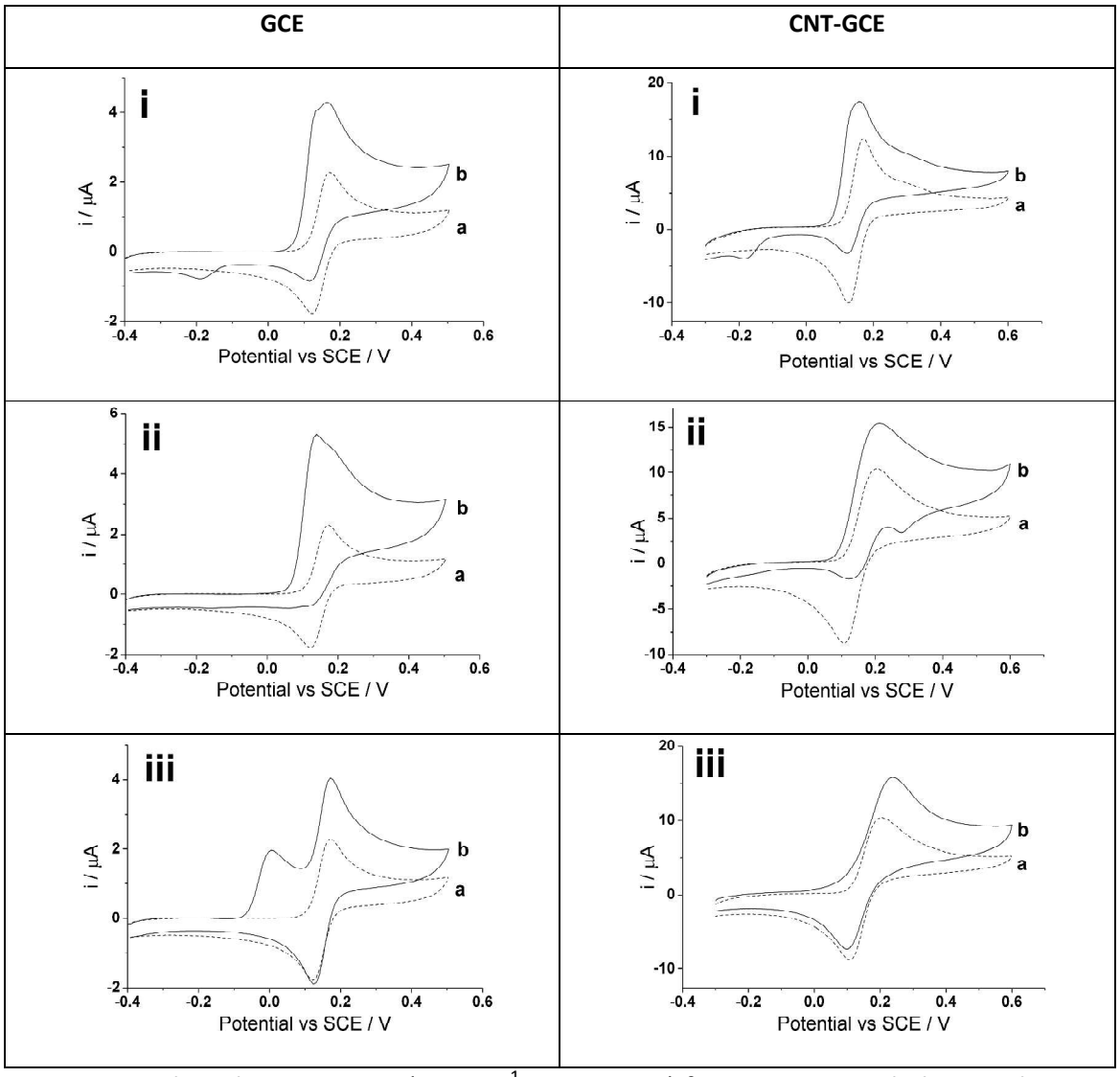

Figure 6. Cyclic voltammograms (50 mVs^{-1}, pH 7.0 PBS) for 0.1 mM catechol in an absence (a) and presence (b) of 0.1 mM concentration of i.) glutathione ii.) cysteine iii.) ascorbic acid at CNT-GCE and GCE.

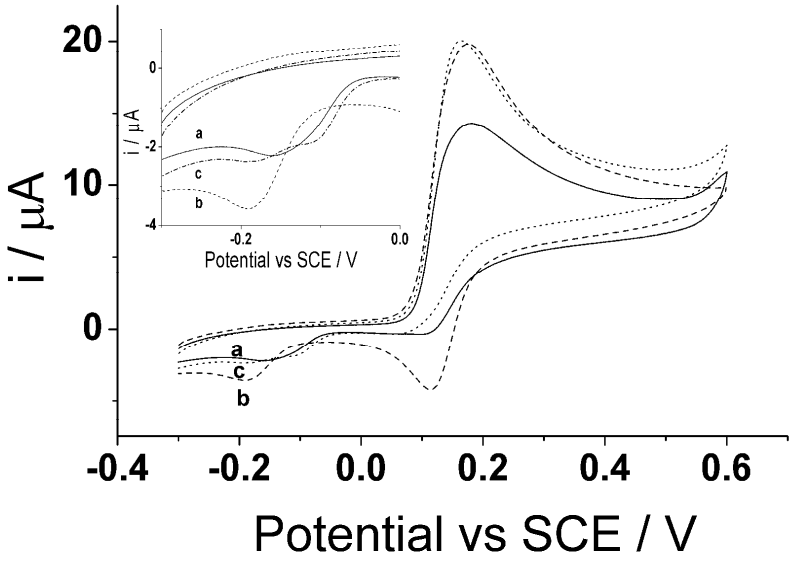

Figure 7. Cyclic voltammograms (50 mVs^{-1}, pH 7.0 PBS) at CNT-GCE of 0.1 mM catechol containing (a) 0.1 mM homocysteine (b) 0.1 mM glutathione and (c) 0.1 mM homocysteine and glutathione.

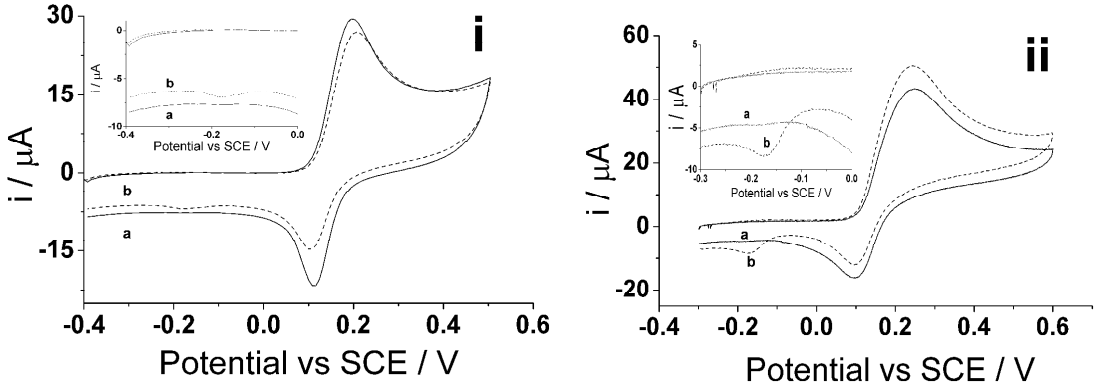

Figure 8. Cyclic voltammograms at i.) GCE (at 1.5 Vs^{-1}) and ii.) CNT-GCE (at 500 mVs-1) of 0.1 mM catechol containing (a) 0.1 mM glutathione and (b) 0.1 mM homocysteine (PBS, pH 7.0).

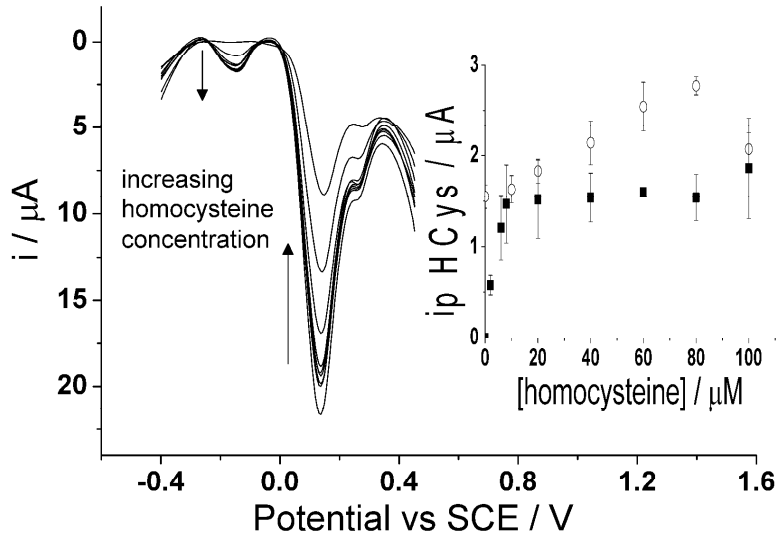

Figure 9. Square wave voltammograms of CNT-GCE in solution containing 0.1 mM glutathione-cysteine-ascorbic acid-catechol with varying homocysteine concentration (0 - 0.1 mM) at 20˚C. *Inset:* Homocysteine peak current at *ca.* - 0.20 V (vs. SCE) plotted against concentration of homocysteine. ■ CNT-GCE and O GCE.

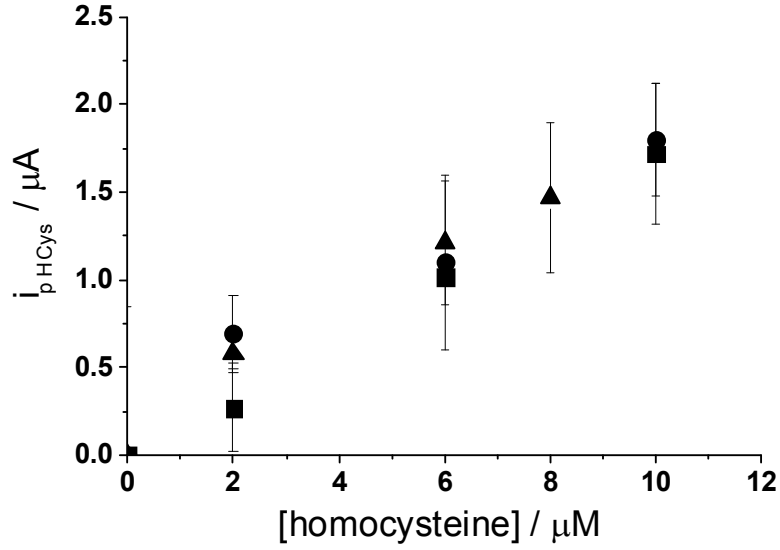

Figure 10. Calibration plot of detection of homocysteine (pH 7.0, PBS at 20˚C) with 0.1 mM catechol present in solution at ■ CNT-GCE. Homocysteine detection in the presence of cysteine, glutathione, and ascorbic acid (PBS, pH 7.0 at 20˚C) at ● CNT-GCE, ▲ CNT-SPE.

Table 1. Tabulated values of antioxidants found in human plasma [14, 22, 30-41] .

Antioxidant Name	Normal Range (μM)	Abnormal Range (μM)
Homocysteine	5 - 15	≥ 100
Cysteine	10 – 30	≥ 100
Glutathione	2 – 12	≥ 100
Ascorbic Acid	30 - 80	0 – 30, 80 - 200

References:

1. G. N. Welch and J. Loscalzo, *New Engl J Med*, 1998, **336**, 1042-1043.
2. E. L. Mayer, D. W. Jacobsen and K. Robinson, *J Am Coll Cardiol*, 1996, **27**, 517-527.
3. H. Refsum, F. Wesenberg and P. M. Ueland, *Cancer Res*, 1991, **51**, 828-835.
4. W. Wang, O. Rusin, X. Xu, K. K. Kim, J. O. Escobedo, S. O. Fakayode, K. A. Fletcher, M. Lowry, C. M. Schowalter, C. M. Lawrence, F. R. Fronczek, I. M. Warner and R. M. Strongin, *J. Am. Chem. Soc.*, 2005, **127**, 15949-15958.
5. W. Wang, J. O. Escobedo, C. M. Lawrence and R. M. Strongin, *J. Am. Chem. Soc.*, 2003, **126**, 3400-3401.
6. K. S. McCully, *Am J Pathol*, 1969, **56**, 111-128.
7. G. J. Hankey and J. W. Eikelboom, *Lancet*, 1999, **354**, 407-413.
8. P. M. Ueland, H. Refrum, S. P. Stabler, M. R. Malinow, A. Andersson and R. H. Allen, *Clin. Chem.*, 1993, **39**, 1764-1779.
9. O. Nekrassova, N. S. Larence and R. G. Compton, *Talanta*, 2003, **60**, 1085-1095.
10. H. Refsum, P. D. Ueland, P. Nygård and S. E. Vollset, *Annu. Rev. Medicine*, 1998, **49**, 31-62.
11. W. Leesutthiphonchai, W. Dungchai, W. Siangproh, N. Ngamrojnavanich and O. Chailapakul, *Talanta*, 2011, **85**, 870-876.
12. B. Hultberg, A. Andersson and A. Isaksson, *Toxicology*, 1997, **123**, 33-40.
13. T. Toyo'oka, *J. Chromatogr.*, 2009, **877**, 3318-3330.
14. A. Pastore, R. Massoud, C. Motti, A. L. Russo, G. Fucci, C. Cortese and G. Federici, *Clin. Chim.* , 1998, **44**, 825-832.
15. S. P. Stabler, P. D. Marcell, E. R. Rodell, R. H. Allen, D. G. Savage and J. Lindenbaum, *J. Clin. Invest.*, 1988, **81**, 466-474.
16. H. Salehzadeh, B. Mokhtari and D. Nematollahi, *Electrochim. Acta*, 2014, **123**, 353-361.
17. N. S. Lawrence, E. L. Beckett, J. Davis and R. G. Compton, *Anal. Biochem.*, 2002, **303**, 1-16.
18. R. W. Murray, A. G. Ewing and R. A. Durst, *Anal. Chem.*, 1987, **59**, 379A-390A.
19. C. A. Thorogood, G. G. Wildgoose, J. H. Jones and R. G. Compton, *New J. Chem.*, 2007, **31**, 958-965.
20. P. T. Lee, K. R. Ward, K. Tschulik, G. Chapman and R. G. Compton, *Electroanal.*, 2014, **26**, 366-373.
21. E. H. Seymour, S. J. Wilkins, N. S. Lawrence and R. G. Compton, *Anal. Lett.*, 2002, **35**, 1387-1399.
22. J. C. Harfield, C. Batchelor-McAuley and R. G. Compton, *Analyst*, 2012, **137**, 2285-2296.
23. P. C. White, N. S. Lawrence, J. Davis and R. G. Compton, *Anal. Chim. Acta*, 2001, **447**, 1-10.
24. L. Fotouhi, L. Behrozi, M. M. Heravi and D. Nematollahi, *Phosphorus Sulfur*, 2009, **184**, 2749-2757.
25. X. Liu, H. Lv, Q. Sun, Y. Zhong, J. Zhao, J. Fu, M. Lin and J. Wang, *Analytical Letters*, 2012, **45**, 2246-2256.
26. DropSens, http://www.dropsens.com/en/home.html. Accessed February 2014.
27. A. Maleki, D. Nematollahi, J. Clausmeyer, J. Henig, N. Plumere and W. Schuhmann, *Electroanal.*, 2012, **24**, 1932-1936.
28. N. S. Lawrence, J. Davies and R. G. Compton, *Talanta*, 2001, **53**, 1089-1094.
29. J. B. Raoof, R. Ojani and D. Nematollahi, *Int. J. Electrochem. Sci.*, 2009, **4**, 810-819.
30. M. A. Mansoor, A. M. Svardal and P. M. Ueland, *Anal. Biochem.*, 1992, **200**, 218-229.
31. W. A. Kleinman and J. P. R. Jr., *Biochem. Pharm.*, 2000, **60**, 19-29.
32. P. C. White, N. S. Lawrence, J. Davis and R. G. Compton, *Electroanal.*, 2002, **14**, 89-98.
33. A. Pastore, G. Federicia, E. Bertinib and F. Piemonteb, *Clin. Chim. Acta*, 2003, **333**, 19-39.
34. S. M. Deneke and B. L. Fanburg, *Am. J. Physiol.*, 1989, **257**, L163-173.

35. D. P. Jones, J. L. Carlson, V. C. M. Jr., J. Cai, M. J. Lynn and P. S. Jr., *Free Radical Biology and Medicine*, 2000, **28**, 625-635.
36. H. Sies, *Free Radical Biology and Medicine*, 1999, **27**, 916-921.
37. F. Michelet, R. Gueguen, P. Leroy, M. Wellman, A. Nicolas and G. Siest, *Gen. Clin. Chem.*, 1995, **41**, 1509-1517.
38. M. Levine, S. J. Padayatty and M. G. Espey, *Adv. Nutr.*, 2011, **2**, 78-88.
39. M. A. Ross, *J. Chromatography B*, 1994, **657**, 197-200.
40. D. J. VanderJagt, P. J. Garry and H. N. Bhaganvan, *Am. J. Clin. Nutr*, 1987, **46**, 290-294.
41. D. Brubacher, U. Mosher and P. Jordan, *Int J Vitam Nutr Res*, 2000, **70**, 225-237.
42. P. C. White, N. S. Lawrence, Y. C. Tsai, J. Davis and R. G. Compton, *Mikrochim. Acta*, 2001, **137**, 87-91.
43. W. Ren, H. Q. Luo and N. B. Li, *Biosens. & Bioelectron.*, 2006, **21**, 1086-1092.
44. M. C. Henstridge, E. J. F. Dickinson, M. Aslanoglu, C. Batchelor-McAuley and R. G. Compton, *Sensor Actuat. B-Chem.*, 2010, **145**, 417-427.
45. M. C. Henstridge, E. J. F. Dickinson and R. G. Compton, *Russian Journal of Electrochemistry*, 2012, **48**, 629-635.